CENTRE FOR **STOCHASTIC GEOMETRY**
AND ADVANCED **BIOIMAGING**

I.T. Andersen and U. Hahn

Matérn thinned Cox processes

No. 08, June 2015

Matérn thinned Cox processes

I.T. Andersen[1,2] and U. Hahn[1]

[1]Department of Mathematics, Aarhus University
[2]Stereological Research Laboratory, Department of Clinical Medicine, Aarhus University

Abstract

A new class of spatial point process models that combines short range repulsion with medium range clustering is introduced. The model is motivated by patterns of centres of non-overlapping spherical cells in biological tissue which tend to have a clustering behaviour. Such a combination of clustering and hard core behaviour can be achieved by applying a dependent Matérn thinning to a Cox process. An exact formula for the intensity of a Matérn thinned shot noise Cox process is derived from the Palm distribution. For the more general class of Matérn thinned Cox processes, formulae for the intensity and second-order characteristics are established using the conditional Poisson assumption. These formulae include more complicated integrals for which approximations are suggested to simplify calculations. An example from pathology illustrates the applicability of the models.

Keywords: Cox process, Dependent thinning, Matérn's hard core process, pair correlation function, Palm retention probability, point process

1 Introduction

The existing point process literature provides models for a variety of interactions between points, of which the models that allow for simple statistical inference often are those used in applications. Most models yield point patterns with either clustering *or* hard core behaviour; however in practical applications, one may observe both types of interaction on different scales simultaneously. One such example is the pattern formed by centres of cells in cell clusters – the centres cannot come closer than the diameter of the cells, but nevertheless they show clustering on a mid range of spatial distance. This example has motivated the present study. In the literature, such cases are often modelled by Gibbs point processes with an appropriate interaction function, as e.g. in Mattfeldt et al. (2006, 2007). While they have an intuitive physical interpretation through the interaction function, theoretical properties and summary statistics of Gibbs models are accessible only by simulation. Another modelling option is to start with a stationary hard core process and obtain a clustered behaviour by independent thinning with probability according to a random field. Second-order summary statistics of these so-called interrupted point processes

(Stoyan, 1979; Lavancier and Møller, 2015) can be obtained straightforwardly from the properties of the hard core process and the random field. In particular if the random field can take zero values, such as a Boolean model, this approach yields a clustered appearance. However, the spatial arrangement of points inside the clusters is influenced by "invisible" points outside the clusters that have been thinned from the original homogeneous pattern, which, depending on the application, may seem less natural from a physical point of view.

In the present paper, we introduce and investigate a new class of mathematically tractable point process models that combine clustering and hard core property, namely by applying dependent Matérn type II thinning (Matérn, 1960, 1986) to a clustered Cox process (Cox, 1955; Møller and Waagepetersen, 2004). In a nutshell, Matérn's thinning algorithms remove points from an existing pattern that have neighbours that are closer than a given hard core distance h. The thinning condition can be interpreted as the condition that balls with diameter h attached to the points may not overlap. In recent years, generalizations of Matérn's hard core models have appeared in the literature. These papers modify the thinning condition, by replacing the non overlapping balls with more general (random) convex sets (Månsson and Rudemo, 2002; Kiderlen and Hörig, 2013), or by thinning according to more general functions of the distance between points (Teichmann et al., 2013), but they still are confined to thinning a homogeneous Poisson point process, as in Matérn's original work. To our knowledge, the Matérn thinning rules have not yet been applied to other point process models. We focus on Cox point processes since they are a very flexible class for clustered patterns, but the general framework of Palm retention probabilities used for calculating first and second order intensities, as derived in Section 3, can directly be applied to other point processes with known Palm distribution.

The paper is organized as follows. In Section 2 we give a short theoretical overview of the applied standard point process models, and we recall some of their properties. In Section 3 we derive general expressions for Palm retention probabilities obtained after a Matérn type II thinning procedure. These probabilities are important in the analysis of Matérn thinned Cox processes, defined in Section 4. Sample realizations and theoretical results with respect to Palm retention probabilities, first- and second-order characteristics of the Matérn thinned Cox processes are also presented in Section 4. Simple approximations are suggested in Section 5, for which the quality is supported by simulations of two examples of Matérn thinned Cox processes, the Matérn thinned Matérn cluster process (MCP) and the Matérn thinned Thomas process (TP). The applicability of the new class of point processes is illustrated in Section 6 by means of an example from pathology of patterns of megakaryocytes in bone marrow. Finally, a short discussion is found in Section 7 and all the included proofs are found in the Appendix.

2 Preliminaries

This section introduces the notation and basic properties of the point process models considered in this paper. References for detailed description of the theory of point processes include Stoyan et al. (1995); Illian et al. (2008); Møller and Waagepetersen (2004).

2.1 Spatial point processes

Let N_{lf} denote the set of locally finite subsets of the d-dimensional Euclidean space $\mathbb{R}^d$, equipped with an appropriate σ-algebra $\mathcal{N}_{\mathrm{lf}}$. Then, *a spatial point process* X is a random variable taking values in N_{lf}. Assume X has well-defined *intensity function* $\rho(\cdot)$ and *second-order product density* $\rho^{(2)}(\cdot,\cdot)$, such that the intensity measure α and the second factorial moment measure $\alpha^{(2)}$ are given by

$$\alpha(B) = \mathbb{E}\Big[\sum_{\xi\in X} \mathbb{1}(\xi \in B)\Big] = \int_B \rho(\xi)\,\mathrm{d}\xi,$$
$$\alpha^{(2)}(B_1 \times B_2) = \mathbb{E}\Big[\sum_{\xi,\eta\in X}^{\neq} \mathbb{1}(\xi \in B_1, \eta \in B_2)\Big] = \int_{B_1}\int_{B_2} \rho^{(2)}(\xi,\eta)\,\mathrm{d}\xi\,\mathrm{d}\eta,$$

for B, B_1 and B_2 in the Borel σ-algebra $\mathcal{B}$ on $\mathbb{R}^d$. Here $\sum^{\neq}$ denotes summation over distinct pairs. The interaction between pairs of points can be described by the *pair correlation function*

$$g(\xi,\eta) = \rho^{(2)}(\xi,\eta)/(\rho(\xi)\rho(\eta)).$$

The process is said to be *stationary* if its distribution is translation invariant. Stationarity implies that the intensity function is constant and that $\rho^{(2)}(\xi,\eta) = \rho^{(2)}(\xi-\eta)$. The process is said to be *isotropic* if its distribution is invariant with respect to rotations around the origin. For stationary and isotropic point processes, we have $\rho^{(2)}(\xi,\eta) = \rho^{(2)}(\|\xi-\eta\|)$. In this case, the pair correlation function is effectively a function on $\mathbb{R}$, $g(r) = \rho^{(2)}(r)/\rho^2, r \in \mathbb{R}$, and the function can be interpreted as the mean number of points at distance r from a "typical" point in X, relative to the mean number for a Poisson process. Here "typical" point is to be understood by means of Palm distribution theory. For the reduced Palm distribution in a point ξ, we will use the notation $\mathbb{P}^!_\xi$, which can be interpreted as the conditional distribution of $X\backslash\xi$ given $\xi \in X$ (Møller and Waagepetersen, 2004, p. 249).

2.2 Cox processes

Let $\{\Lambda(x)\}$ be a non-negative random field, which is almost surely locally integrable with respect to the Lebesgue measure. A point process X is by definition a *Cox process with driving field* Λ, if conditionally on Λ, X is a Poisson process with intensity function Λ (Cox, 1955; Møller and Waagepetersen, 2004). It follows from the conditional behaviour of X, that the intensity function and the second-order product density are given by

$$\rho(x) = \mathbb{E}[\Lambda(x)] \quad \text{and} \quad \rho^{(2)}(x,y) = \mathbb{E}[\Lambda(x)\Lambda(y)]. \tag{2.1}$$

Furthermore, the *void probability* for bounded $B \in \mathcal{B}$ is given by

$$\mathbb{P}(X \cap B = \emptyset) = \mathbb{E}\Big[\exp\Big(-\int_B \Lambda(\xi)\,\mathrm{d}\xi\Big)\Big], \tag{2.2}$$

and the *generating functional* $G_X(f) = \mathbb{E}[\prod_{\xi\in X} f(\xi)]$ for a function $f : \mathbb{R}^d \to [0,1]$ is

$$G_X(f) = \mathbb{E}\Big[\exp\Big(-\int_{\mathbb{R}^d}(1-f(\xi))\Lambda(\xi)\,\mathrm{d}\xi\Big)\Big], \tag{2.3}$$

cf. Møller and Waagepetersen (2004, p. 60). A Cox process is stationary and isotropic if the driving field Λ is stationary and isotropic.

Shot noise Cox processes (SNCPs) are characterized by random intensity functions of the form

$$\Lambda(\xi) = \sum_{(c,\gamma)\in\Phi} \gamma k(c,\xi), \tag{2.4}$$

where Φ is a Poisson process of cluster centres and cluster intensities on $\mathbb{R}^d \times (0,\infty)$ with a locally finite diffuse intensity measure denoted by ζ, and $k(c,\cdot)$ is a kernel, i.e. a probability density function on $\mathbb{R}^d$. See more details in Møller (2003). SNCPs can be regarded as *Poisson cluster processes*, as $X|\Phi$ is distributed as the superposition of independent Poisson processes $X_{(c,\gamma)}$, $(c,\gamma) \in \Phi$, with intensity functions $\gamma k(c,\cdot)$.

Neyman-Scott processes (NSPs) (Neyman and Scott, 1958), which are also Cox processes, can be regarded as a particular case of SNCPs with constant γ in (2.4). In the stationary case, Λ takes the form

$$\Lambda(\xi) = \sum_{c\in C} \mu k(\xi - c), \tag{2.5}$$

where C is a stationary Poisson process on $\mathbb{R}^d$ with intensity $\kappa > 0$, say. The intensity for a stationary NSP is $\rho = \mu\kappa$. Two examples of well-known stationary NSPs are given below. These processes will be used throughout the paper to show how the general formulas simplifies in concrete examples.

Example 1 (Matérn cluster process)**.** *A simple and popular NSP is the Matérn cluster process (MCP) (Matérn, 1960, 1986), where the kernel*

$$k(\xi) = \mathbb{1}(\|\xi\| \le R)/|b(o,R)|$$

is the uniform density on a ball $b(o,R)$ centered at the origin and of radius $R > 0$. Here and in the following, $|B|$ denotes the volume of a set B. Note that a MCP is distributed as $\bigcup_{c\in C} X_c$, where $X_c|C$ is a stationary Poisson point process on $b(c,R)$ with mean number of points $\mu > 0$, and where X_c, $c \in C$, are mutually independent and independent of C.

Example 2 (Thomas process)**.** *The class of NSPs also includes Thomas processes (TPs) (Thomas, 1949), where the kernel*

$$k(\xi) = \exp(-\|\xi\|^2/2\sigma^2)/(2\pi\sigma^2)^{d/2}$$

is the density for d independent normally distributed variables with mean 0 and variance $\sigma^2 > 0$. As for the MCP, the TP can be constructed as a Poisson cluster process.

The reduced Palm distribution $\mathbb{P}_\xi^!$ of a SNCP takes a particularly simple form, as it is just the distribution of X superposed with an independent cluster containing ξ. This turns out to be useful in the following sections. The result is restated below. The proof may be found in Møller (2003, Proposition 2).

Proposition 1 (Reduced Palm distribution of SNCPs)**.** *Let X be a SNCP with random intensity of the form* (2.4)*. For $\rho(\xi) > 0$, let*

$$\Lambda_\xi(\eta) = \gamma_\xi k(c_\xi, \eta), \quad \eta \in \mathbb{R}^d,$$

where (c_ξ, γ_ξ) is a random variable with distribution

$$\mathbb{P}((c_\xi, \gamma_\xi) \in D) = \frac{\int_D \gamma k(c, \xi)\, \mathrm{d}\zeta(c, \gamma)}{\rho(\xi)}, \quad \text{for Borel sets } D \subseteq \mathbb{R}^d \times (0, \infty).$$

Let $X_\xi | (c_\xi, \gamma_\xi)$ be a Poisson process with intensity function Λ_ξ and let $(c_\xi, \gamma_\xi, X_\xi)$ be independent of (Φ, X). Then, for Lebesgue almost all ξ with $\rho(\xi) > 0$,

$$\mathbb{P}_\xi^!(F) = \mathbb{P}(X \cup X_\xi \in F), \quad F \in \mathcal{N}_{\mathrm{lf}}.$$

2.3 Matérn's hard core models

Matérn (1960, 1986) introduced three hard core models, obtained by dependent thinning of a stationary Poisson process, according to a hard core distance $h > 0$. These models are known as Matérn's processes of types I, II and III. The most simple model, based on Matérn type I thinning, solely depends on the point configuration of the original process. All points with a neighbour closer than the distance h are deleted, and this thinning rule results in the most sparse process. In contrast, the most popular thinning algorithm, the Matérn type II thinning, depends also on independent "arrival time" marks, which are attached to the points of the original Poisson process. The hard core property is then achieved by removing points if there are other points within a distance h with a smaller mark. Naturally, the intensity of the type II model becomes higher than that for the type I model. To increase the intensity further, Matérn proposed an iterative procedure, where a point is only influenced by other points that have not already been deleted (type III model). Due to the resulting long range dependence, closed forms for the summary statistics of the type III model do not exist, and therefore we only consider Matérn type II thinning in this paper.

3 Palm retention probabilities for Matérn type II thinned processes

An important tool in analysing the Matérn thinned Cox processes is calculation of Palm retention probabilities. They have the intuitive interpretation as the probability that a given point (or a pair of points) that is present in the original pattern "survives" the thinning. In this section, we derive expressions for these probabilities, valid for an arbitrary point process X.

Let the mark attached to a point $\xi \in X$ of the point process be denoted m_ξ. The marks are assumed independent, continuously and identically distributed, and independent of X. Without loss of generality, the marks will be assumed to be uniformly distributed on $[0, 1)$ (Stoyan and Stoyan, 1985). Let $X_M = \{(\xi, m_\xi) | \xi \in X, m_\xi \sim \text{unif}[0, 1)\}$ denote the marked process. The Matérn type II thinned process is then given by

$$\text{MatII}(X_M; h) \coloneqq \{\xi \in X \mid \forall (\eta, m_\eta) \in X_M, \eta \neq \xi : \|\xi - \eta\| > h \vee m_\eta > m_\xi\}. \quad (3.1)$$

The ratio between the intensity function ρ_{th} of the thinned process $X_{\text{th}} = \text{MatII}(X_M; h)$ and the intensity function ρ of the original process X can be interpreted as a retention probability

$$p_{\text{ret}}(\xi) \coloneqq \rho_{\text{th}}(\xi)/\rho(\xi). \quad (3.2)$$

The probability will be called the *Palm retention probability*, since it can be expressed in terms of the reduced Palm distribution $\mathbb{P}^!_{(\xi, m_\xi)}$ for the marked process X_M. In fact,

$$p_{\text{ret}}(\xi) = \int_0^1 p_{\text{ret}}(\xi, m_\xi) \, \mathrm{d}m_\xi, \quad (3.3)$$

where

$$p_{\text{ret}}(\xi, m_\xi) = \mathbb{P}^!_{(\xi, m_\xi)}(F(\xi, m_\xi; h)), \quad (3.4)$$

and $F(\xi, m_\xi; h)$ is the set of marked point patterns x_M, for which the point ξ with mark m_ξ is retained in the thinned process,

$$F(\xi, m_\xi; h) \coloneqq \{x_M \mid \forall (\eta, m_\eta) \in x_M : \|\xi - \eta\| > h \vee m_\eta > m_\xi\}.$$

A proof of (3.3) can be found in the Appendix.

Second- and higher-order Palm retention probabilities can be treated analogously. Let $\rho^{(2)}_{\text{th}}$ and $\rho^{(2)}$ denote the second-order product density of X_{th} and X, respectively. Then, the second-order retention probability is defined by

$$p^{(2)}_{\text{ret}}(\xi, \eta) \coloneqq \rho^{(2)}_{th}(\xi, \eta)/\rho^{(2)}(\xi, \eta). \quad (3.5)$$

As in (3.3) and (3.4), we have

$$p^{(2)}_{\text{ret}}(\xi, \eta) = \int_0^1 \int_0^1 p^{(2)}_{\text{ret}}((\xi, m_\xi)(\eta, m_\eta)) \, \mathrm{d}m_\xi \, \mathrm{d}m_\eta \quad (3.6)$$

with

$$p^{(2)}_{\text{ret}}((\xi, m_\xi), (\eta, m_\eta)) = \mathbb{1}(\|\xi - \eta\| > h) \mathbb{P}^!_{(\xi, m_\xi), (\eta, m_\eta)}(F(\xi, m_\xi; h) \cap F(\eta, m_\eta; h)). \quad (3.7)$$

Here, $\mathbb{P}^!_{(\xi, m_\xi)(\eta, m_\eta)}$ is the two-point reduced Palm distribution for X_M (Hanisch, 1982, p. 172). A proof of (3.6) can be found in the Appendix.

In cases where it is possible to calculate the retention probabilities, the intensity and second-order product density of the thinned process can be obtained by multiplying the ones for the original process with the retention probabilities. If X_{th} is obtained by thinning a stationary and isotropic point process X, X_{th} will likewise be stationary and isotropic, and the intensity and second-order product density are given by

$$\rho_{\text{th}} = p_{\text{ret}} \rho \quad \text{and} \quad \rho^{(2)}_{\text{th}}(r) = p^{(2)}_{\text{ret}}(r) \rho^{(2)}(r). \quad (3.8)$$

4 Matérn thinned Cox processes

A Matérn (type II) thinned Cox process is defined as follows.

Definition 1. *A Matérn thinned Cox process with parameters* (Λ, h) *is a point process given by*

$$\mathrm{MTCP}(\Lambda, h) \coloneqq \{\xi \in X \mid \forall (\eta, m_\eta) \in X_M, \eta \neq \xi : \|\xi - \eta\| > h \vee m_\eta > m_\xi\}, \quad (4.1)$$

where X *is a Cox process with driving field* Λ *and* $X_M = \{(\xi, m_\xi) \mid \xi \in X, m_\xi \sim \mathrm{unif}[0,1)\}$ *is the marked process with i.i.d. uniform marks.*

Sample realizations of Matérn thinned MCPs and TPs in $\mathbb{R}^2$ are shown in Figure 1.

For Matérn thinned Cox processes, there exist (at least) two possible methods to derive the intensity function and the second-order product density for the thinned process. Either one can try to calculate the retention probabilities in (3.3) and (3.6) directly, or one can use the standard approach for Cox processes, and first condition on the random intensity function, and then calculate the retention probabilities given the random intensity function. The first approach is in general more difficult, but as we shall see in Theorem 2 below it is possible to find explicit expressions for the first-order retention probability for Matérn thinned SNCPs. A proof of Theorem 2 can be found in the Appendix.

Theorem 2 (Retention probabilities of Matérn thinned SNCPs)**.** *The first-order Palm retention probability* (3.3) *of* $\mathrm{MTCP}(\Lambda, h)$ *with shot noise driving field* Λ *specified by* (2.4) *is given by*

$$p_{\mathrm{ret}}(\xi) = \int_0^1 \exp\Big(-\int_{\mathbb{R}^d \times (0,\infty)} p_{\xi,m}(c,\gamma)\,\mathrm{d}\zeta(c,\gamma)\Big) \times \Big(\int_{\mathbb{R}^d \times (0,\infty)} \gamma(1 - p_{\xi,m}(c,\gamma))\frac{k(c,\xi)}{\rho(\xi)}\,\mathrm{d}\zeta(c,\gamma)\Big)\,\mathrm{d}m,$$

where

$$p_{\xi,m}(c,\gamma) = 1 - \exp\Big(-m\int_{b(\xi,h)} \gamma k(c,\eta)\,\mathrm{d}\eta\Big).$$

From Theorem 2 we can easily derive the retention probabilities for Matérn thinned NSPs.

Corollary 3 (Retention probabilities of Matérn thinned NSPs)**.** *The first-order Palm retention probability* (3.3) *of* $\mathrm{MTCP}(\Lambda, h)$ *with Neyman-Scott driving field* Λ *specified by* (2.5) *with* $\mu, \kappa > 0$ *is given by*

$$p_{\mathrm{ret}} = \int_0^1 \exp\Big(-\kappa\int_{\mathbb{R}^d} p_m(c)\,\mathrm{d}c\Big)\Big(\int_{\mathbb{R}^d}(1 - p_m(c))k(-c)\,\mathrm{d}c\Big)\,\mathrm{d}m,$$

where

$$p_m(c) = 1 - \exp\Big(-\mu m\int_{b(o,h)} k(\eta - c)\,\mathrm{d}\eta\Big).$$

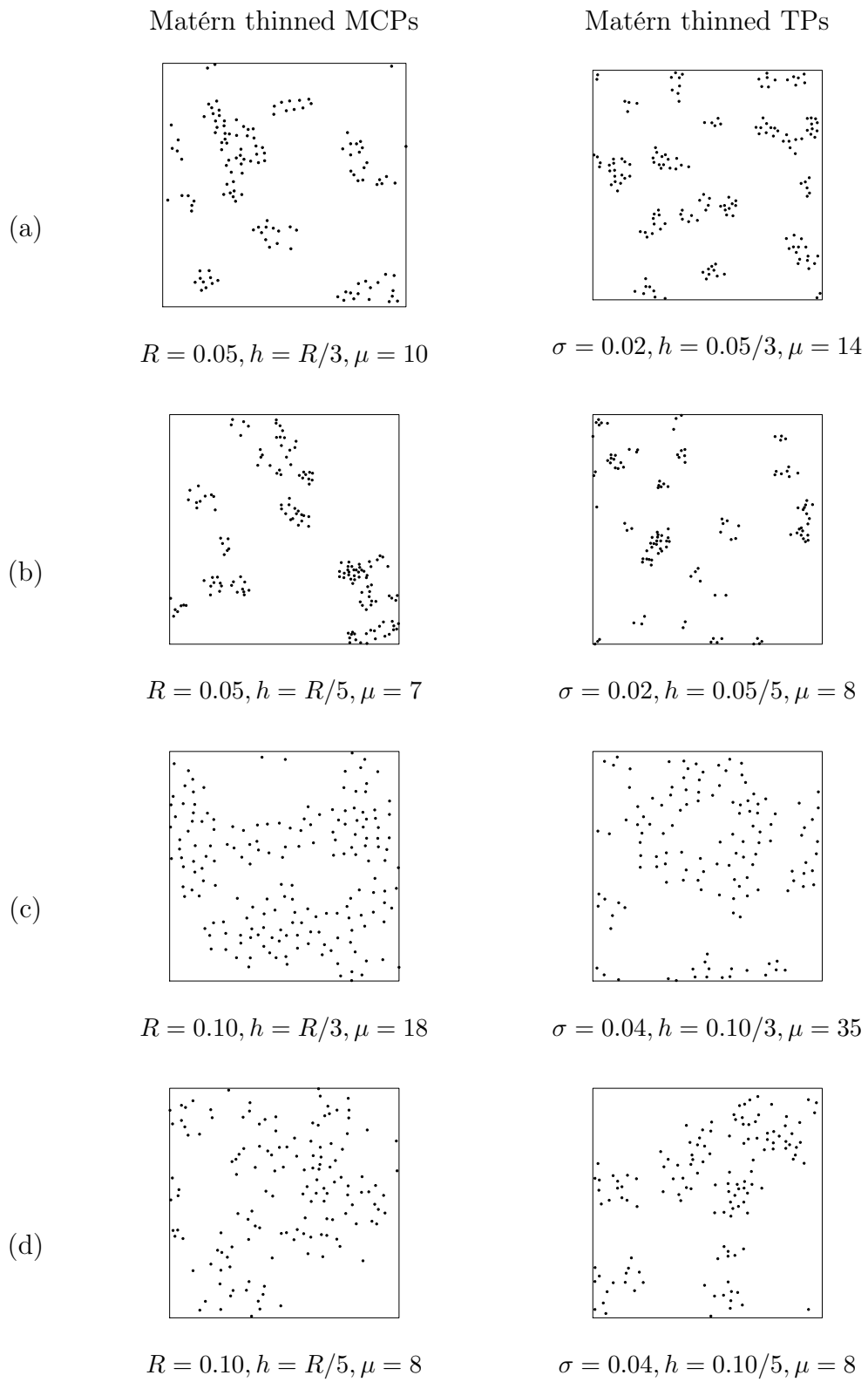

Figure 1: Sample realizations of Matérn thinned MCPs (left) and Matérn thinned TPs (right) in observation window $W = [0, 1]^2$, with four choices of parameters, all with intensities $\rho_{\text{th}} \approx 150$ and $\kappa = 25$.

Further simplifications are possible in the case of isotropy, which is illustrated in Example 3 and 4 for the Matérn thinned MCPs and Matérn thinned TPs, respectively.

Example 3 (Example 1, continued)**.** *For $d = 2$, the first-order Palm retention probability of a Matérn thinned MCP reduces to*

$$p_{\mathrm{ret}} = \int_0^1 \exp\Big(-2\pi\kappa \int_0^{R+h} p_m(r) r \,\mathrm{d}r\Big)\Big(2/R^2 \int_0^R (1 - p_m(r)) r \,\mathrm{d}r\Big)\,\mathrm{d}m, \tag{4.2}$$

where

$$p_m(r) = p_m(\|\xi_r\|) = 1 - \exp(-\mu\, m|b(o,h) \cap b(\xi_r, R)|/(\pi R^2)).$$

Example 4 (Example 2, continued)**.** *For $d = 2$, the first-order Palm retention probability of a Matérn thinned TP reduces to*

$$p_{\mathrm{ret}} = \int_0^1 \exp\Big(-2\pi\kappa \int_0^{\infty} p_m(r) r \,\mathrm{d}r\Big) \times \Big(1/\sigma^2 \int_0^{\infty} (1 - p_m(r)) \exp(-r^2/(2\sigma^2)) r \,\mathrm{d}r\Big)\,\mathrm{d}m, \tag{4.3}$$

where

$$p_m(r) = 1 - \exp\Big(-\mu\, m/(2\pi\sigma^2) \times \int_{-h}^{h} \int_{-\sqrt{h^2-\eta_2^2}}^{\sqrt{h^2-\eta_2^2}} \exp(-(\eta_1^2 + (\eta_2 - r)^2)/(2\sigma^2))\,\mathrm{d}\eta_1\,\mathrm{d}\eta_2\Big).$$

For general Matérn thinned Cox processes the intensity function and the second-order product density can be determined by conditioning on the random intensity function.

Theorem 4 (Intensity function and second-order produkt density of Matérn thinned Cox processes)**.** *Assume Λ is a driving field of a Cox process that almost surely fulfils*

$$\Lambda(\xi) > 0 \quad \Rightarrow \quad \int_{b(\xi,r)} \Lambda(\eta)\,\mathrm{d}\eta > 0, \quad \textit{for all } r > 0, \tag{4.4}$$

which can be regarded as the assumption, that the random intensity function almost surely has no singularities.

Then for $\mathrm{MTCP}(\Lambda, h)$*, the intensity function and second-order product density are given by*

$$\rho_{\mathrm{th}}(\xi) = \mathbb{E}\big[p_{\mathrm{ret}|\Lambda}(\xi)\Lambda(\xi)\big] \tag{4.5}$$

and

$$\rho^{(2)}_{\mathrm{th}}(\xi,\eta) = \mathbb{E}\big[p^{(2)}_{\mathrm{ret}|\Lambda}(\xi,\eta)\Lambda(\xi)\Lambda(\eta)\big] \tag{4.6}$$

for $\|\xi - \eta\| > h$*, otherwise 0, where for* $\Lambda(\xi)$ *and* $\Lambda(\eta) > 0$*,*

$$p_{\mathrm{ret}|\Lambda}(\xi) = \tfrac{1-\exp(-\Omega_\xi)}{\Omega_\xi} \tag{4.7}$$

and

$$p^{(2)}_{\mathrm{ret}|\Lambda}(\xi,\eta) = \tfrac{1-\exp(-\Omega_\xi)}{\Omega_\xi \Omega_{\eta\setminus\xi}} + \tfrac{1-\exp(-\Omega_\eta)}{\Omega_\eta \Omega_{\xi\setminus\eta}} - \tfrac{1-\exp(-\Omega_{\xi\cup\eta})}{\Omega_{\xi\cup\eta}}\Big(\tfrac{1}{\Omega_{\xi\setminus\eta}} + \tfrac{1}{\Omega_{\eta\setminus\xi}}\Big), \tag{4.8}$$

with $\Omega_* = \int_{b_*} \Lambda(\tau)\,\mathrm{d}\tau$*, and* $b_\xi = b(\xi,h)$*,* $b_{\xi\setminus\eta} = b(\xi,h)\setminus b(\eta,h)$*, and* $b_{\xi\cup\eta} = b(\xi,h)\cup b(\eta,h)$*.*

A proof of Theorem 4 may be found in the Appendix. If the original process is an inhomogeneous Poisson process (corresponding to a Cox process case, where $\Lambda(\xi) = \rho(\xi)$ is deterministic), the retention probabilities reduce to

$$p_{\mathrm{ret}}(\xi) = \frac{1-\exp(-\omega_\xi)}{\omega_\xi} \tag{4.9}$$

and

$$p^{(2)}_{\mathrm{ret}}(\xi,\eta) = \tfrac{1-\exp(-\omega_\xi)}{\omega_\xi \omega_{\eta\setminus\xi}} + \tfrac{1-\exp(-\omega_\eta)}{\omega_\eta \omega_{\xi\setminus\eta}} - \Big(\tfrac{1-\exp(-\omega_{\xi\cup\eta})}{\omega_{\xi\cup\eta}}\Big)\Big(\tfrac{1}{\omega_{\xi\setminus\eta}} + \tfrac{1}{\omega_{\eta\setminus\xi}}\Big) \tag{4.10}$$

for $\|\xi - \eta\| > h$, otherwise 0, where $\omega_* = \int_{b_*} \rho(\vartheta)\,\mathrm{d}\vartheta$ and b_ξ is defined in Theorem 4.

In the stationary and isotropic case (corresponding to the Matérn type II model), the intensity is given by

$$\rho_{\mathrm{th}} = \frac{1-\exp(-\rho\tau_h)}{\tau_h}, \tag{4.11}$$

and the second-order product density is given by

$$\rho^{(2)}_{\mathrm{th}}(r) = \begin{cases} 0, & r \le h, \\ \dfrac{2\Gamma_h(r)(1-\exp(-\rho\tau_h)) - 2\tau_h(1-\exp(-\mu\Gamma_h(r)))}{\tau_h\Gamma_h(r)(\Gamma_h(r)-\tau_h)}, & r > h, \end{cases} \tag{4.12}$$

where ρ is the intensity of the process before thinning, $\tau_h = |b(o,h)|$, $\Gamma_h(r) = |b(o,h)\cup b(\xi_r,h)|$, $\xi_r \in \mathbb{R}^d$ with $\|\xi_r\| = r$. These formulas may also be found in e.g. Matérn (1960) and Stoyan et al. (1995).

5 First- and second-order approximations

5.1 Derivation of approximations

The expected values in the expressions for $\rho_{\mathrm{th}}(\xi)$ and $\rho^{(2)}_{\mathrm{th}}(\xi,\eta)$, given by Equations (4.5) and (4.6) in Theorem 4, are in general hard to calculate explicitly. Therefore, it can be useful to derive approximations. We will approximate the intensity function and second-order product density of a Matérn thinned Cox process by

$$\rho_{\mathrm{a}}(\xi) \coloneqq \mathbb{E}[p_{\mathrm{a}|\Lambda}(\xi)\Lambda(\xi)], \tag{5.1}$$

and

$$\rho_{\mathrm{a}}^{(2)}(\xi,\eta) \coloneqq \mathbb{E}[p_{\mathrm{a}|\Lambda}^{(2)}(\xi,\eta)\Lambda(\xi)\Lambda(\eta)], \tag{5.2}$$

for $\|\xi-\eta\| > h$, otherwise 0, where $p_{\mathrm{a}|\Lambda}(\xi)$ and $p_{\mathrm{a}|\Lambda}^{(2)}(\xi,\eta)$ are obtained by replacing Ω_* in the retention probabilities (4.7) and (4.8) with the following approximations

$$\Omega_\xi = \int_{b(\xi,h)} \Lambda(\vartheta)d\vartheta \approx \Lambda(\xi)\tau_h, \tag{5.3}$$

$$\Omega_{\xi\cup\eta} = \int_{b(\xi,h)\cup b(\eta,h)} \Lambda(\vartheta)d\vartheta \approx (\Lambda(\xi)+\Lambda(\eta))\Gamma_h(r)/2, \tag{5.4}$$

$$\Omega_{\xi\setminus\eta} = \int_{b(\xi,h)\setminus b(\eta,h)} \Lambda(\vartheta)d\vartheta \approx \Lambda(\xi)(\Gamma_h(r)-\tau_h), \tag{5.5}$$

where $r = \|\xi-\eta\|$, $\tau_h = |b(o,h)|$, $\Gamma_h(r) = |b(o,h)\cup b(\xi_r,h)|$, $\xi_r \in \mathbb{R}^d$, with $\|\xi_r\| = r$. Simple formulas for the approximated intensity function and second-order product density can then be found.

Theorem 5 (First- and second-order approximations for Matérn thinned Cox processes)**.** *The approximated intensity function and second-order product density of a* MTCP(Λ,h)*, defined by* (5.1) *and* (5.2)*, are given by*

$$\rho_{\mathrm{a}}(\xi) = \tfrac{1-\mathbb{E}[\exp(-\Lambda(\xi)\tau_h)]}{\tau_h} \tag{5.6}$$

and

$$\rho_{\mathrm{a}}^{(2)}(\xi,\eta) = \tfrac{\Gamma_h(r)(2-\mathbb{E}[\exp(-\Lambda(\xi)\tau_h)]-\mathbb{E}[\exp(-\Lambda(\eta)\tau_h)])-2\tau_h(1-\mathbb{E}[\exp(-(\Lambda(\xi)+\Lambda(\eta))\Gamma_h(r)/2)])}{\tau_h\Gamma_h(r)(\Gamma_h(r)-\tau_h)} \tag{5.7}$$

for $\|\xi-\eta\| = r > h$, otherwise 0.

The proof of Theorem 5 may be found in the Appendix. From Theorem 5 we can derive the approximated intensity function and second-order product density for Matérn thinned SNCPs.

Corollary 6 (First- and second-order approximations for Matérn thinned SNCPs)**.** *For SNCPs with driving field Λ given by* (2.4)*, the expected values in Theorem 5 are for $\|\xi-\eta\| = r$ given by*

$$\mathbb{E}[\exp(-\Lambda(\xi)\tau_h)] = \exp(-a(\xi)), \tag{5.8}$$

$$\mathbb{E}[\exp(-(\Lambda(\xi)+\Lambda(\eta))\Gamma_h(r)/2)] = \exp(-b(\xi,\eta)), \tag{5.9}$$

where

$$a(\xi) = \int_{\mathbb{R}^d\times(0,\infty)} (1-\exp(-\gamma k(c,\xi)\tau_h))\,\mathrm{d}\zeta(c,\gamma),$$

$$b(\xi,\eta) = \int_{\mathbb{R}^d\times(0,\infty)} (1-\exp(-\gamma\{k(c,\xi)+k(c,\eta)\}\Gamma_h(r)/2))\,\mathrm{d}\zeta(c,\gamma).$$

For stationary Matérn thinned NSPs with driving field Λ given by (2.5), $a(\xi)$ and $b(\xi,\eta)$ reduce to

$$a = \kappa \int_{\mathbb{R}^d} (1 - \exp(-\mu k(\vartheta)\tau_h))\,\mathrm{d}\vartheta,$$
$$b(\xi-\eta) = \kappa \int_{\mathbb{R}^d} (1 - \exp(-\mu\{k(\xi-\eta+\vartheta)+k(\vartheta)\}\Gamma_h(r)/2))\,\mathrm{d}\vartheta.$$

The formulas become particularly simple for stationary and isotropic Matérn thinned NSPs, which is illustrated in Example 5 and 6 for Matérn thinned MCPs and Matérn thinned TPs in the plane.

Example 5 (Example 1, continued)**.** *For $d = 2$, $k(\xi) = \mathbb{1}(\|\xi\| \le R)/(\pi R^2)$ and $b(\xi-\eta) = b(\|\xi-\eta\|)$, say, a and b in Corollary 6 for Matérn thinned MCPs reduce to*

$$\begin{aligned} a &= \kappa\pi R^2(1-\exp(-\mu h^2/R^2)) \text{ and} \\ b(r) &= 2\kappa(1-\exp(-\mu\Gamma_h(r)/(2\pi R^2)))(\Gamma_R(r)-\pi R^2) \\ &\quad + \kappa(1-\exp(-\mu\Gamma_h(r)/(\pi R^2)))(2\pi R^2 - \Gamma_R(r)). \end{aligned}$$

Example 6 (Example 2, continued)**.** *For $d = 2$, $k(\xi) = \exp(-\|\xi\|^2/(2\sigma^2))/(2\tau_\sigma)$ and $b(\xi-\eta) = b(\|\xi-\eta\|)$, say, a and b in Corollary 6 for Matérn thinned TPs reduce to*

$$a = 2\pi\kappa \int_0^\infty (1 - \exp[-\mu\, h^2/(2\sigma^2)\exp(-r^2/(2\sigma^2))])r\,\mathrm{d}r,$$
$$\begin{aligned} b(r) = \kappa \int_{\mathbb{R}}\int_{\mathbb{R}} &(1-\exp(-\mu\{\exp(-(\vartheta_1^2+\vartheta_2^2)/(2\sigma^2))+ \\ &\exp(-(\vartheta_1^2+(\vartheta_2-r)^2)/(2\sigma^2))\}\Gamma_h(r)/(4\pi\sigma^2)))\,\mathrm{d}\vartheta_1\,\mathrm{d}\vartheta_2. \end{aligned}$$

Combining Theorem 5 and Corollary 6, the approximated intensity function and the second-order product density for stationary and isotropic Matérn thinned NSPs simplify to

$$\rho_{\mathrm{a}} = \frac{1-\exp(-a)}{\tau_h}, \tag{5.10}$$

and for $r > h$,

$$\rho_{\mathrm{a}}^{(2)}(r) = \frac{2\Gamma_h(r)(1-\exp(-a)) - 2\tau_h(1-\exp(-b(r)))}{\tau_h\Gamma_h(r)(\Gamma_h(r)-\tau_h)}. \tag{5.11}$$

The approximated pair correlation function is defined by $g_{\mathrm{a}}(\xi,\eta) \coloneqq \rho_{\mathrm{a}}^{(2)}(\xi,\eta)/(\rho_{\mathrm{a}}(\xi)\rho_{\mathrm{a}}(\eta))$. For stationary and isotropic Matérn thinned NSPs, we find

$$g_{\mathrm{a}}(r) = \frac{\rho_{\mathrm{a}}^{(2)}(r)}{\rho_{\mathrm{a}}^2} = \frac{2\Gamma_h(r)\tau_h(1-\exp(-a)) - 2\tau_h^2(1-\exp(-b(r)))}{\Gamma_h(r)(\Gamma_h(r)-\tau_h)(1-\exp(-a))^2}. \tag{5.12}$$

5.2 Properties of the approximations in Matérn thinned MCPs and Matérn thinned TPs.

In order to examine the quality of the approximations ρ_{a} and g_a in (5.10) and (5.12), Matérn thinned MCPs and Matérn thinned TPs have been considered in the plane for different combinations of the parameters.

The approximated intensity ρ_{a} is compared to the theoretical intensity $\rho_{\mathrm{th}} = p_{\mathrm{ret}}\rho$, where p_{ret} is found from (4.2) in Example 3 for Matérn thinned MCPs and (4.3) in Example 4 for Matérn thinned TPs (obtained by numerical integration). The results are summarized in Figure 2, which shows the relative bias as a function of the hard core distance h, relative to the cluster radius R, for the nine combinations of parameters (κ, μ) indicated in the figure. For Matérn thinned MCPs, R is simply the radius for which the kernel is positive, while for the Matérn thinned TPs, R is determined such that

$$\int_{\mathbb{R}^2} k(\|\xi\|)\mathbb{1}(\|\xi\| \leq R)\,\mathrm{d}\xi \approx 95\%.$$

For Matérn thinned MCPs, ρ_{a} yields a negative, but relatively small bias, when h is reasonable small compared to R. For Matérn thinned TPs, ρ_{a} approximates ρ_{th} very well. To asses the quality of the approximation for the pair correlation function (pcf), g_a is compared to an estimated theoretical pcf obtained by averaging 500 empirical estimates from sample realizations. We consider four combinations of parameter values for each of the two types of processes, Matérn thinned MCPs and Matérn thinned TPs. See Figure 1 for parameter details and sample realizations.

For the simulated point patterns from each of the chosen combinations of parameters, non-parametric estimates $\hat{g}(r)$ of the pcfs were found using the `pcf.ppp` function from the `spatstat` package in R (Baddeley and Turner, 2005), with default values of r, the Epanechnikov kernel, fixed kernel bandwidth parameter `bw` $= h/\sqrt{5}$, `translate` for the choice of edge correction and `divisor = d`. Since the estimator $\hat{g}(r)$ is based on kernel smoothing, it is biased. In particular, it will assign values $\hat{g}(r) > 0$ for $r < h$. One can show that $\hat{g}(r)$ with the above choice of parameters is a ratio unbiased estimator for the convolution of the true pair correlation function with the kernel, see Fiksel (1988). We therefore consider the kernel smoothed version

$$\widetilde{g_{\mathrm{a}}}(r) := \int g_{\mathrm{a}}(s)k(r-s)ds \tag{5.13}$$

when judging the quality of approximation by simulation.

In Figure 3, g_{a} and $\widetilde{g_{\mathrm{a}}}$ are compared to estimated pcfs for Matérn thinned MCPs (left) and Matérn thinned TPs (right). The grey areas mark pointwise central 95%-regions. The black full drawn lines are the average estimated pcfs, and the red stippled and full drawn lines represent g_{a} and $\widetilde{g_{\mathrm{a}}}$, respectively. The smooth versions $\widetilde{g_{\mathrm{a}}}$ of g_{a} are very similar to the average estimated pcfs in all cases considered, in particular for the Matérn thinned MCPs.

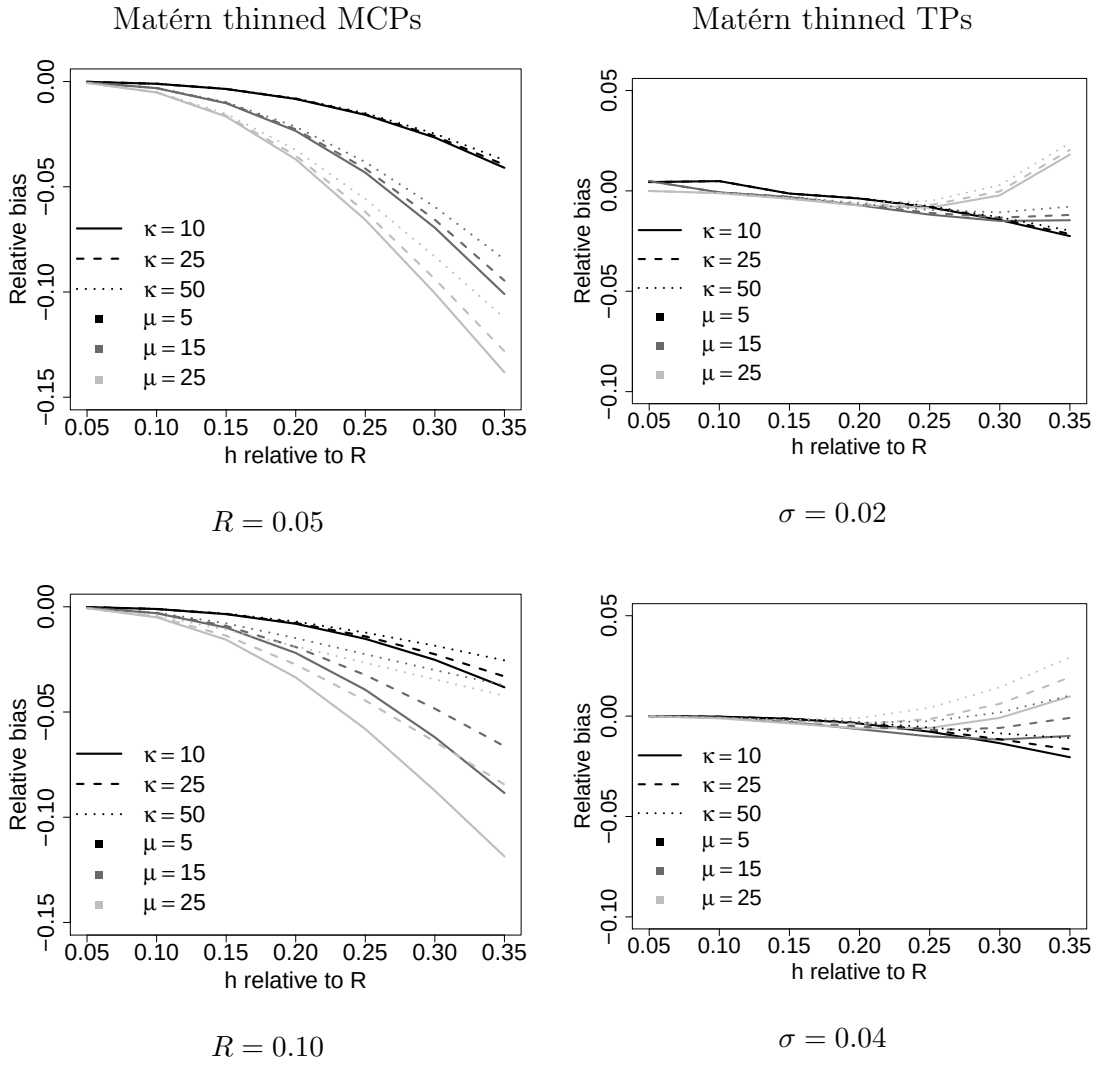

Figure 2: The relative bias of the approximated intensities of Matérn thinned MCPs (left) and Matérn thinned TPs (right) from the theoretical intensities obtained by numerical integration. The bias is shown as a function of the hard core distance h, relative to the cluster radius R. For Matérn thinned MCPs, R is simply the radius for which the kernel is positive, while for Matérn thinned TPs, a comparable R is used. For details, see text. In each sub-figure, nine different models are considered, corresponding to all the combinations of three cluster intensities, $\kappa = 10$, 25 and 50 (unbroken, dashed and dotted lines, respectively), and three mean number of points in a cluster before thinning, $\mu = 5$, 15 and 25 (black, dark grey and light grey lines, respectively).

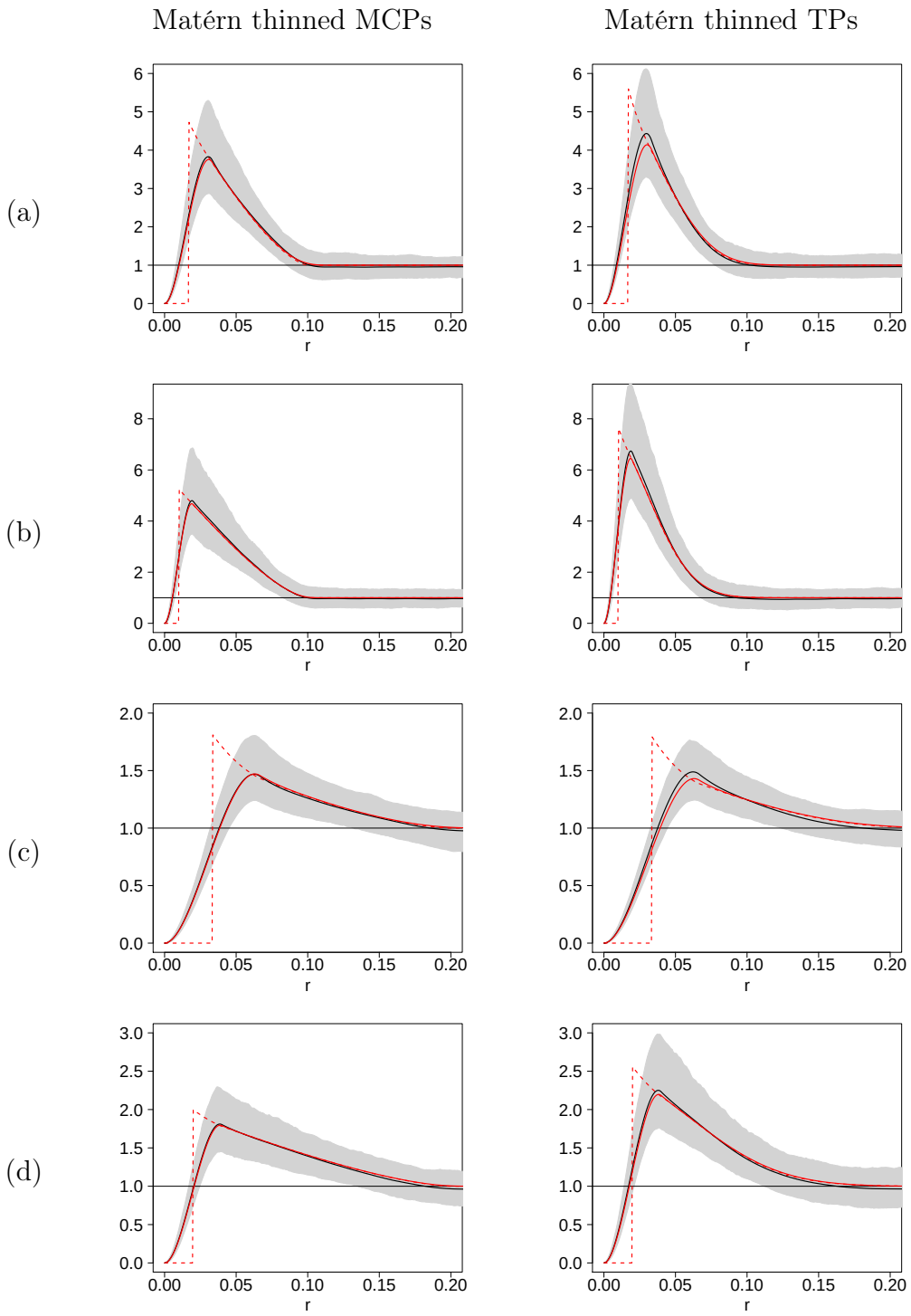

Figure 3: For Matérn thinned MCPs (left) and Matérn thinned TPs (right) and each of the parameter combinations (a)-(d) shown in Figure 1, estimates of the pcfs are shown together with the approximated pcfs g_a (red stippled lines). The estimates of the pcfs are represented by the grey areas, which mark pointwise central 95%-regions, based on 500 simulations. The average pcfs, based on these simulations, are also shown (black full drawn lines) as well as the smooth versions $\widetilde{g}_{\mathrm{a}}$ of g_{a} (red full drawn lines).

6 Applications

In this section, we consider point patterns describing the position of megakaryocytes in bone marrow biopsy sections for a control group and three case groups with hematopoietic stemcell disorders, essential thrombocythemia (ET), polycythemia vera (PV) and primary myelofibrosis (PMF). The diseases result in an increased number of megakaryocytes and different levels of clustering, which is used as diagnostic indicators in pathology. Pathologists determine the level of clustering (i.e. no, "loose" and "dense" clustering) by a visual judgement following different vaguely described rules, see e.g. Madelung et al. (2013); Vytrva et al. (2014) for further details. To the best of our knowledge, no precise quantitative measure for the degree of clustering between megakaryocytes has been used in the existing literature within the field of pathology and this is therefore the first time, point process theory has been applied to measure the level of clustering in this application.

Megakaryocytes are large cells, which are easy to distinguish from other cells. See Figure 4 for an illustrative example of megakaryocytes at high magnification. We considered 1, 5, 3 and 4 biopsies for the control, ET, PMF and PV group, respectively. One section per biopsy was scanned and divided into sub-sections, resulting in 9, 13, 10 and 10 sub-sections, respectively. These were chosen as parts of the sections, where the tissue was fairly regular and unbroken. For the case groups, the sub-sections were of size $1540\,\mu\text{m} \times 1540\,\mu\text{m}$, but for the control group we chose parts of different sizes to include enough cells for the point process analysis. In Figure 5, sub-section examples are shown for the four groups, where the tissue and megakaryocytes have been outlined. The distinct clustering behaviour and low density in the pattern formed by the centres of the megakaryocyte profiles suggest that Matérn thinned Cox processes are suitable models. In order to reveal differences between the groups, we fitted Matérn thinned MCPs and Matérn thinned TPs to the data. The hard core distance h is considered as a nuisance parameter. Considering minimum point-to-point distances, we chose $h = 25\,\mu\text{m}$. A preliminary investigation showed that the results were not affected substantially by choosing other reasonable values of h. To estimate the other model parameters, we applied the minimum contrast method in combination with the pcf (Diggle, 1983, Chapter 6). More concretely, the estimated parameter vector $\hat{\theta}$ is found by a search algorithm as the minimizer of the discrepancy measure

$$D(\theta) = \int_{r_1}^{r_2} (\hat{g}(r)^q - g(r;\theta)^q)^2 \,\mathrm{d}r$$

between the theoretical function $g(\cdot;\theta)$ and its empirical non-parametric counterpart $\hat{g}$, where r_1, r_2 and q are tuning parameters specified below. We estimated the pair correlation functions for each group as average of pcfs estimated on the sub-sections, using `spatstat` as described in Section 5.2. To avoid bias due to kernel estimation, we replaced the theoretical pcf with the convoluted version $\widetilde{g}_{\text{a}}$ given in (5.13). The set of candidate parameters for the search of $\hat{\theta}$ was restricted to parameters that yield an approximated intensity ρ_{a} calculated from (5.10) to be equal to the observed one.

The tuning parameters were set to $r_1 = 0$, $r_2 = 200\,\mu\text{m}$, and $q = 1$. The value of

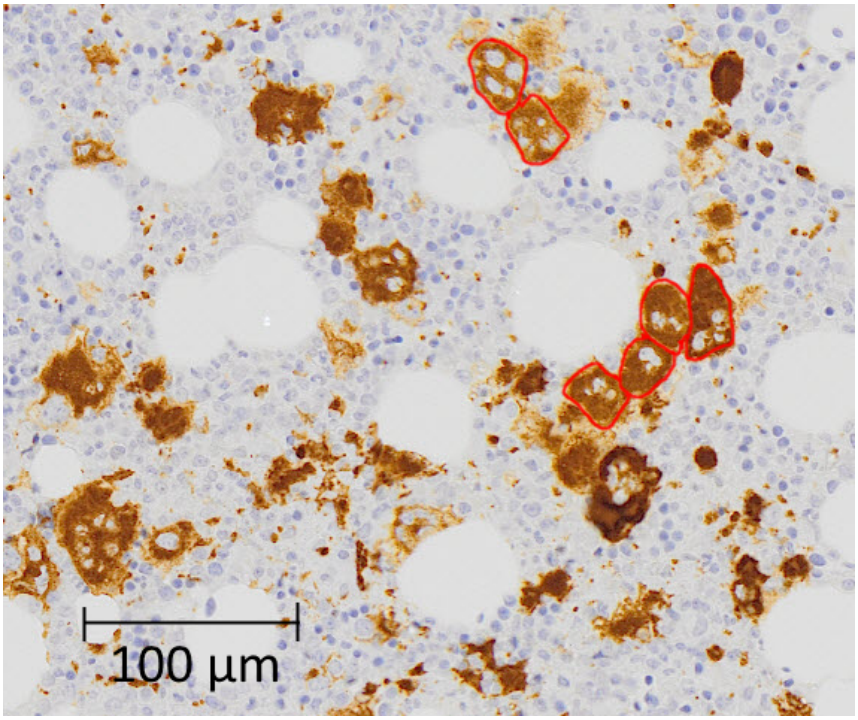

Figure 4: A small part of a bone marrow biopsy section at high magnification. The bone marrow consists mostly of blood forming cells, among them megakaryocytes, a few of which have been outlined with red. On the section, huge white fat cells are also seen.

q can be used to add weight to the part of the functions most important for the analysis. The short range clustering seem to be of most importance in the pathological application, thus we chose $q = 1$.

In Table 1 an overview of the fitted parameters are given for the Matérn thinned MCP and Matérn thinned TP models. Besides the model parameters we also show the usual non-parametric estimate for the intensity $\hat{\rho}_{\text{th}} = \#\text{Cell}/|W|$, the estimate for the mean number of cells in a cluster after thinning $\hat{\mu}_{\text{th}} = \hat{\rho}_{\text{th}}/\hat{\kappa}$ and the discrepancy measure.

In Figure 6, we consider the four groups (top to bottom) and the fitted Matérn thinned MCPs (left) and Matérn thinned TPs (right). The estimated pcf for each group from the observed point patterns are shown as black full drawn lines. The approximated pcfs g_a for the Matérn thinned MCPs and Matérn thinned TPs with fitted parameters are also shown, as well as the smooth versions $\widetilde{g}_{\text{a}}$ (red stippled and full drawn lines, respectively). The grey areas mark pointwise central 95%-regions based on 500 simulations from the fitted Matérn thinned MCPs and Matérn thinned TPs.

The fitted Matérn thinned MCPs and Matérn thinned TPs seem to capture most of the behaviour of the pcfs from the observed point pattern, although we see that the models slightly underestimate the level of clustering for short and large range distances and slightly overestimate the level of clustering for medium range distances. The Matérn thinned TPs result in slightly better fit, except for the PV group, where the models are almost equally good (see the discrepancy measure in Table 1).

All groups indicate a clustering behaviour, but the control group can easily be distinguished from the case groups due to the low intensity. The PMF group is the most clustered group and seems to have a much higher mean number of cells per cluster than the rest of the groups. The ET and PV group show similar behaviour of the pcfs, with ET having slightly smaller clusters with fewer cells per cluster.

Table 1: Estimated parameters from fitting Matérn thinned MCPs and Matérn thinned TPs to the observed point patterns using the estimated pcf for each group. Besides the model parameters we also estimated the following quantities: the usual non-parametric estimate for the intensity $\hat{\rho}_{\text{th}} = \#\text{Cell}/|W|$, the estimate for the mean number of cells in a cluster after thinning $\hat{\mu}_{\text{th}} = \hat{\rho}_{\text{th}}/\hat{\kappa}$ and the discrepancy measure.

Estimated parameters	Groups and Matérn thinned models							
	Control		ET		PMF		PV	
	MC	T	MC	T	MC	T	MC	T
$\hat{\kappa} \times 10^5$ (per (µm)^2)	3.95	3.44	2.59	2.57	1.48	1.48	2.38	2.39
$\hat{R}$ or $\hat{\sigma}$ (µm)	56.3	34.8	86.8	45.7	76.4	38.6	113	59.3
$\hat{\mu}$	0.43	0.48	1.54	1.54	4.16	4.11	2.47	2.50
$\hat{\rho}_{\text{th}} \times 10^5$ (per (µm)^2)	1.58	1.58	3.62	3.62	4.74	4.74	5.25	5.25
$\hat{\mu}_{\text{th}}$	0.40	0.46	1.40	1.41	3.21	3.21	2.21	2.20
Discrepancy measure	2.57	2.16	0.50	0.37	2.82	1.98	0.40	0.41

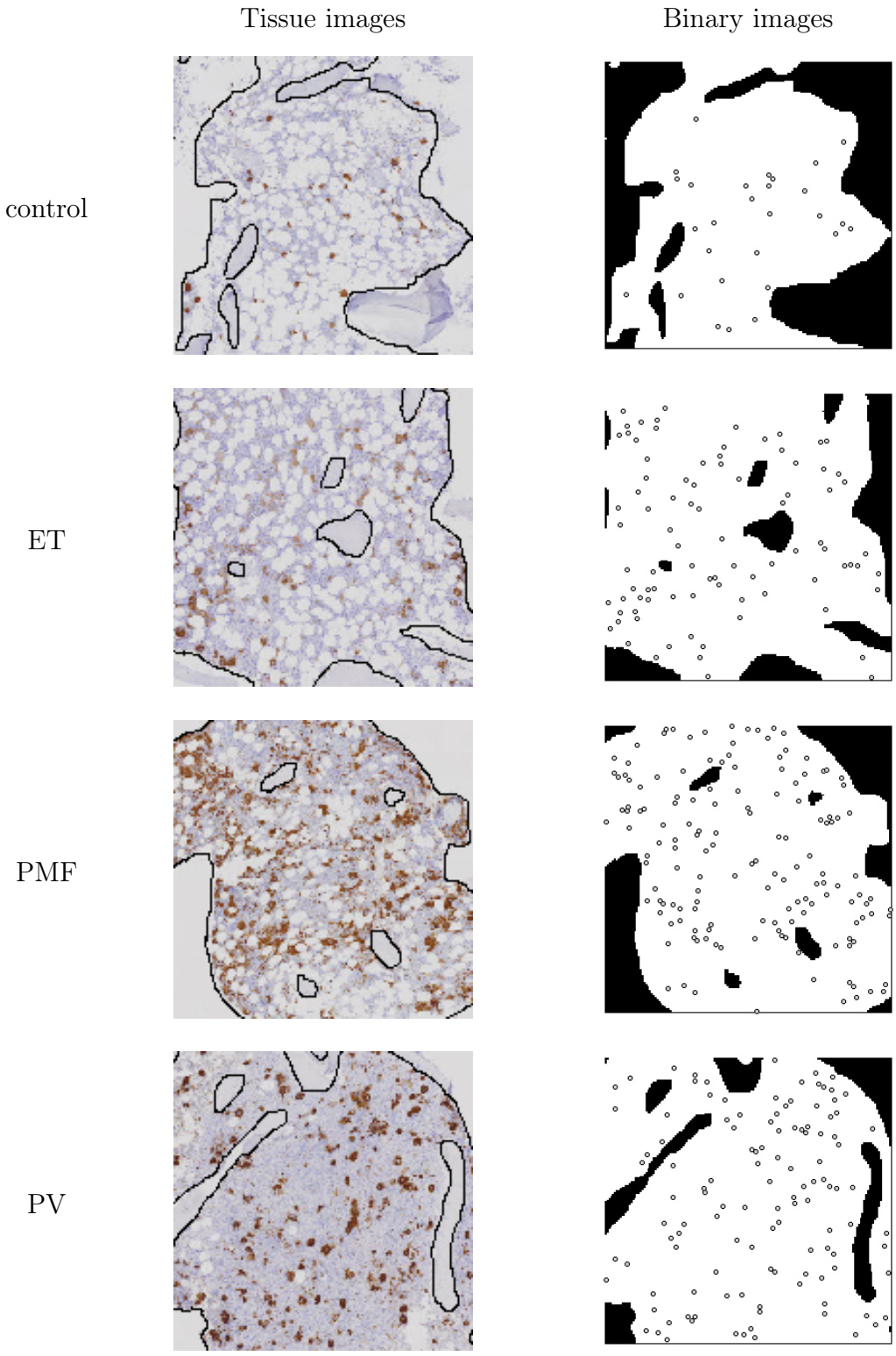

Figure 5: Sub-section examples (1540 µm × 1540 µm) of the control, ET, PMF and PV group. Tissue images and binary images are shown, where the tissue and cells have been marked. The cells have been marked manually and they are represented by balls of radius $r = h/2 = 12.5\,\mu\text{m}$.

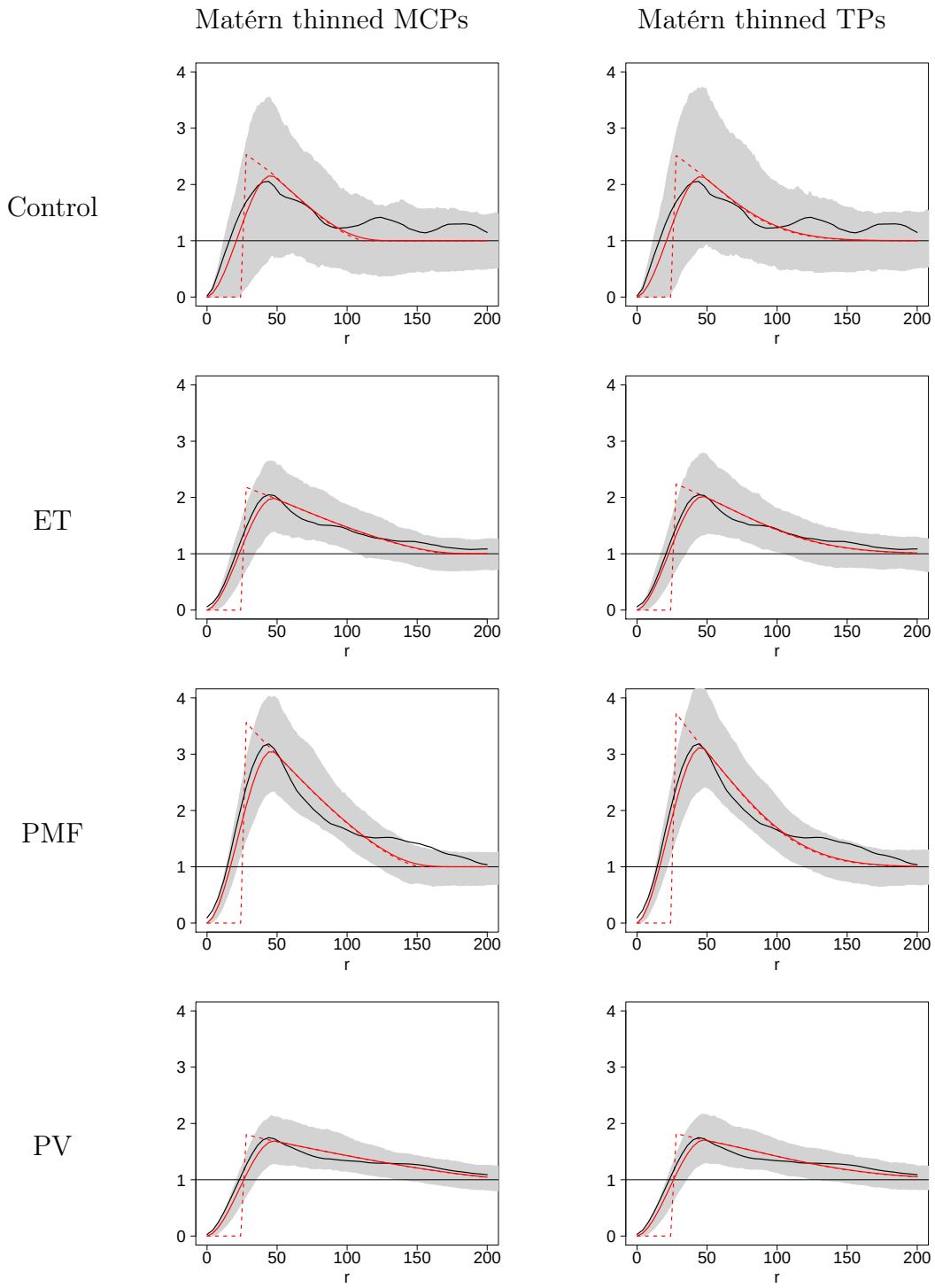

Figure 6: Group estimated pcfs from the observed point patterns are shown (black full drawn lines) for the control, ET, PMF and PV group. The approximated pcfs as well as the ones after smoothing (see details in the text) of the fitted models are shown (red stippled and full drawn lines, respectively) for Matérn thinned MCPs (left) and Matérn thinned TPs (right). The grey areas mark pointwise central 95%-regions based on 500 simulations from the fitted models.

7 Discussion

In the present paper, we have defined the new class of Matérn thinned Cox processes and derived formulae for first- and second-order characteristics. Furthermore, we have suggested approximations to simplify calculations. For Matérn thinned MCPs and Matérn thinned TPs, the accuracy of the approximations were examined by numerical integration (for the intensity) and by simulations (for the pair correlation function), which indicates that the approximations capture most of the true behaviour of the models. The approximations enable simple fitting of the models, using e.g. the minimum contrast method, without the need of simulations. Model fitting using both Matérn thinned MCPs and Matérn thinned TPs were performed in a study of the pattern of megakaryocytes under different diseases. The models fitted very well the observed behaviour of the estimated pcfs, resulting in a valid analysis procedure to detect clustering of these cells, which is missing in the literature within the field of pathology. As only a pilot study with few sections was available, a future larger study must be performed to establish more robust conclusions for the groups under considerations. The fitted Matérn thinned MCPs and Matérn thinned TPs are very similar, and as numerical integration is only necessary for the approximations of the more complicated Matérn thinned TPs, the Matérn thinned MCPs could very well be preferred.

There are still some open questions regarding the approximations. It may be possible to obtain results regarding upper bounds for the deviation between the theoretical and approximated quantities. Furthermore, a thorough, future simulation study of the Matérn thinned Cox processes is needed to investigate in detail for which choices of parameters efficient estimation of the parameters is possible.

8 Acknowledgement

The authors would like to thank Ann Brinch Madelung and Jens R. Nyengaard for their expertise regarding the practical application, and are indebted to Ann Brinch Madelung for the days spent in the laboratory counting the cells. The authors are very grateful to Eva B. Vedel Jensen for her thorough comments and constructive ideas for the manuscript. This research was supported by the Centre for Stochastic Geometry and Advanced Bioimaging, funded by the Villum Foundation.

A Proofs

PROOF OF (3.3). To show (3.3), let $X_{M\mathrm{th}}$ denote the thinned marked process. Then, the intensity measure of X_{th} is for $B \in \mathcal{B}$ given by

$$\alpha_{X_{\mathrm{th}}}(B) = \alpha_{X_{M\mathrm{th}}}(B \times [0,1)) = \mathbb{E} \sum_{(\xi,m_\xi)\in X_M} h((\xi,m_\xi), X_M \backslash (\xi,m_\xi)),$$

where

$$h((\xi,m_\xi), X_M\backslash(\xi,m_\xi)) = \mathbb{1}(\xi \in B)\mathbb{1}(X_M\backslash(\xi,m_\xi) \in F(\xi,m_\xi;h)).$$

Applying the Campbell-Mecke theorem (Møller and Waagepetersen, 2004, p. 249) on the marked process X_M and the function $h((\xi,m_\xi), X_M\backslash(\xi,m_\xi))$, we obtain

$$\alpha_{\mathrm{th}}(B) = \int_B \int_0^1 \mathbb{P}^!_{(\xi,m_\xi)}(F(\xi,m_\xi;h))\,\mathrm{d}m_\xi\,\rho(\xi)\,\mathrm{d}\xi.$$

This equality holds for all $B \in \mathcal{B}$, and therefore we have $\rho_{\mathrm{th}}(\xi) = p_{\mathrm{ret}}(\xi)\rho(\xi)$ for Lebesgue almost all ξ, where $p_{\mathrm{ret}}(\xi)$ is given by (3.3). □

PROOF OF (3.6). To derive (3.6), we rewrite the second factorial moment measure of the thinned process for $B_1, B_2 \in \mathcal{B}$

$$\alpha^{(2)}_{\mathrm{th}}(B_1 \times B_2) = \mathbb{E} \sum^{\neq}_{(\xi,m_\xi),(\eta,m_\eta)\in X_M} h((\xi,m_\xi),(\eta,m_\eta), X_M\backslash\{(\xi,m_\xi),(\eta,m_\eta)\}),$$

where

$$\begin{aligned} &h((\xi,m_\xi),(\eta,m_\eta), X_M\backslash\{(\xi,m_\xi),(\eta,m_\eta)\}) \\ &\quad = \mathbb{1}((\xi,\eta) \in B_1 \times B_2)\mathbb{1}(\|\xi-\eta\| > h)\mathbb{1}(X_M\backslash\{(\xi,m_\xi),(\eta,m_\eta)\} \\ &\quad \in F(\xi,m_\xi;h) \cap F(\eta,m_\eta;h)). \end{aligned}$$

Using Hanisch (1982, (2.4) and (2.6)) with $n = 2$, we find

$$\begin{aligned} &\alpha^{(2)}_{\mathrm{th}}(B_1 \times B_2) \\ &\quad = \int_{\mathbb{R}^d}\int_{\mathbb{R}^d}\int_0^1\int_0^1 \mathbb{E}^!_{(\xi,m_\xi)(\eta,m_\eta)}\, h((\xi,m_\xi),(\eta,m_\eta),X_M)\alpha^{(2)}_M(\mathrm{d}(\xi,m_\xi),\mathrm{d}(\eta,m_\eta)). \end{aligned}$$

Since $\alpha^{(2)}_M(\mathrm{d}(\xi,m_\xi),\mathrm{d}(\eta,m_\eta)) = \rho^{(2)}(\xi,\eta)\,\mathrm{d}m_\xi\,\mathrm{d}m_\eta\,\mathrm{d}\xi\,\mathrm{d}\eta$, we get (3.6). □

PROOF OF THEOREM 2. Recall that $X = \bigcup_{(c,\gamma)\in\Phi} X_{(c,\gamma)}$, where Φ is a Poisson process and $X_{(c,\gamma)}|\Phi$ are independent Poisson processes on $\mathbb{R}^d$ with intensity functions $\gamma k(c,\cdot)$.

The marked process $X_M = \{(\xi,m_\xi) \mid \xi \in X, m_\xi \sim \mathrm{unif}[0,1)\}$ can then similarly be written as $X_M = \bigcup_{(c,\gamma)\in\Phi} X_{(c,\gamma)M}$, where $X_{(c,\gamma)M} = \{(\xi,m_\xi) \mid \xi \in X_{(c,\gamma)}, m_\xi \sim \mathrm{unif}[0,1)\}$ and $X_{(c,\gamma)M}|\Phi$ are independent Poisson processes on $\mathbb{R}^d \times [0,1)$ with intensity functions $h_{(c,\gamma)}(\xi,m) = \gamma k(c,\xi)$ for all $(c,\gamma) \in \Phi$. Thus, X_M is again a SNCP,

and the retention probability can be obtained using Proposition 1 on the marked SNCP X_M.

Let $X_{M(\xi,m)}$ denote the random process specified in Proposition 1. Then by definition $X_{M(\xi,m)}|(c_{\xi,m},\gamma_{\xi,m})$ is a Poisson process with intensity function $\Lambda_{\xi,m}(\eta,\tilde{m}) = \gamma_{\xi,m}k(c_{\xi,m},\eta)$, the distribution of $(c_{\xi,m},\gamma_{\xi,m})$ is given by

$$\mathbb{P}((c_{\xi,m},\gamma_{\xi,m})\in D) = \frac{\int_D \gamma k(c,\xi)\,\mathrm{d}\zeta(c,\gamma)}{\rho(\xi)}, \quad \text{for Borel sets } D\subseteq \mathbb{R}^d\times(0,\infty),$$

and $(c_{\xi,m},\gamma_{\xi,m},X_{M(\xi,m)})$ is independent of (Φ,X_M). Next, we notice that

$$F(\xi,m;h) = \{x_M \mid x_M\cap(b(\xi,h)\times[0,m]) = \emptyset\}.$$

Using the simple description of the reduced Palm distribution in Proposition 1, we obtain

$$\begin{aligned} p_{\mathrm{ret}}(\xi,m) &= \mathbb{P}^!_{(\xi,m)}(F(\xi,m;h)) \\ &= \mathbb{P}(X_M\cap(b(\xi,h)\times[0,m]) = \emptyset)\mathbb{P}(X_{M(\xi,m)}\cap(b(\xi,h)\times[0,m]) = \emptyset), \end{aligned}$$

where the void probabilities are

$$\mathbb{P}(X_M\cap(b(\xi,h)\times[0,m]) = \emptyset) = \exp\Big(-\int_{\mathbb{R}^d\times(0,\infty)} p_{\xi,m}(c,\gamma)\,\mathrm{d}\zeta(c,\gamma)\Big), \tag{A.1}$$

$$\mathbb{P}(X_{M(\xi,m)}\cap(b(\xi,h)\times[0,m]) = \emptyset) = \int_{\mathbb{R}^d\times(0,\infty)} \gamma(1-p_{\xi,m}(c,\gamma))\frac{k(c,\xi)}{\rho(\xi)}\,\mathrm{d}\zeta(c,\gamma), \tag{A.2}$$

with

$$p_{\xi,m}(c,\gamma) = 1-\exp\Big(-m\int_{b(\xi,h)}\gamma k(c,\eta)\,\mathrm{d}\eta\Big). \tag{A.3}$$

The result in (A.1) follows by using that X_M is a SNCP together with (2.2) and (2.3) in the Poisson case. The result in (A.2) is derived using Proposition 1 as follows

$$\begin{aligned} &\mathbb{P}(X_{M(\xi,m)}\cap(b(\xi,h)\times[0,m]) = \emptyset) \\ &\quad= \mathbb{E}\,\mathbb{P}(X_{M(\xi,m)}\cap(b(\xi,h)\times[0,m]) = \emptyset|(c_{\xi,m},\gamma_{\xi,m})) \\ &\quad= \mathbb{E}\Big[\exp\Big(-m\int_{b(\xi,h)}\gamma_{\xi,m}k(c_{\xi,m},\eta)\,\mathrm{d}\eta\Big)\Big] \\ &\quad= \int_{\mathbb{R}^d\times(0,\infty)}\gamma(1-p_{\xi,m}(c,\gamma))\frac{k(c,\xi)}{\rho(\xi)}\,\mathrm{d}\zeta(c,\gamma). \end{aligned}$$

□

Proof of Theorem 4. The intensity function and the second-order product density of X_{th} can be written as

$$\begin{aligned} \rho_{\mathrm{th}}(\xi) &= \mathbb{E}\Big[\Lambda_{\mathrm{th}}(\xi)\Big], \\ \rho^{(2)}_{\mathrm{th}}(\xi,\eta) &= \mathbb{E}\Big[\Lambda^{(2)}_{\mathrm{th}}(\xi,\eta)\Big], \end{aligned}$$

where $\Lambda_{\text{th}}(\xi)$ and $\Lambda^{(2)}_{\text{th}}(\xi,\eta)$ are the intensity function and second-order product density function of X_{th} given Λ. Using (3.2) and (3.5), we get that

$$\Lambda_{\text{th}}(\xi) = p_{\text{ret}|\Lambda}(\xi)\Lambda(\xi),$$
$$\Lambda^{(2)}_{\text{th}}(\xi,\eta) = p^{(2)}_{\text{ret}|\Lambda}(\xi,\eta)\Lambda(\xi)\Lambda(\eta).$$

To find $p_{\text{ret}|\Lambda}(\xi)$ and $p^{(2)}_{\text{ret}|\Lambda}(\xi,\eta)$ it remains to derive the retention probabilities for inhomogeneous Poisson processes.

Let $\mathbb{P}^!_{(\xi,m_\xi)|\Lambda}$ be the reduced Palm distribution for the marked point process X_M given Λ. Using (3.3), we find

$$p_{\text{ret}|\Lambda}(\xi) = \int_0^1 \mathbb{P}^!_{(\xi,m_\xi)|\Lambda}(F(\xi,m_\xi;h))\,\mathrm{d}m_\xi. \tag{A.4}$$

Since the conditional distribution of X_M given Λ is inhomogeneous Poisson with intensity function $\Lambda_M(\xi,m_\xi) = \Lambda(\xi)$, we can use the Slivnyak-Mecke theorem (Møller and Waagepetersen, 2004, (3.7)), and get

$$\mathbb{P}^!_{(\xi,m_\xi)|\Lambda}(F(\xi,m_\xi;h)) = \mathbb{P}(X_M \cap (b(\xi,h)\times[0,m_\xi]) = \emptyset|\Lambda) = \exp(-\Omega_\xi m_\xi).$$

Inserting in (A.4), we get (4.7).

Likewise, using (3.6), we find

$$p^{(2)}_{\text{ret}}(\xi,\eta) = \int_0^1\int_0^1 \mathbb{1}(\|\xi-\eta\|>h)\mathbb{P}^!_{(\xi,m_\xi),(\eta,m_\eta)|\Lambda}(F(\xi,m_\xi;h)\cap F(\eta,m_\eta;h))\,\mathrm{d}m_\xi\,\mathrm{d}m_\eta,$$

where

$$\begin{aligned}
&\mathbb{P}^!_{(\xi,m_\xi),(\eta,m_\eta)|\Lambda}(F(\xi,m_\xi;h)\cap F(\eta,m_\eta;h))\\
&\quad= \mathbb{P}(X_M\cap(b(\xi,h)\times[0,m_\xi])=\emptyset, X_M\cap(b(\eta,h)\times[0,m_\eta])=\emptyset|\Lambda)\\
&\quad= \exp(-(\Omega_{\xi\setminus\eta}m_\xi + \Omega_{\eta\setminus\xi}m_\eta + \Omega_{\xi\cap\eta}(m_\xi\vee m_\eta)),
\end{aligned}$$

for $\|\xi-\eta\|>h$, otherwise 0, for which (4.8) similarly appears from integration over the marks. □

Proof of Theorem 5. Let $\Lambda(\xi)$, $\Lambda(\eta)>0$, and $\|\xi-\eta\|=r$. Using the approximations (5.3)-(5.5), the approximated retention probabilities reduce to

$$p_{\text{a}|\Lambda}(\xi) = \tfrac{1-\exp(-\Lambda(\xi)\tau_h)}{\Lambda(\xi)\tau_h}$$

and

$$\begin{aligned}
p^{(2)}_{\text{a}|\Lambda}(\xi,\eta) &= \tfrac{1-\exp(-\Lambda(\xi)\tau_h)}{\Lambda(\xi)\tau_h\Lambda(\eta)(\Gamma_h(r)-\tau_h)} + \tfrac{1-\exp(-\Lambda(\eta)\tau_h)}{\Lambda(\eta)\tau_h\Lambda(\xi)(\Gamma_h(r)-\tau_h)}\\
&\quad - \tfrac{1-\exp(-(\Lambda(\xi)+\Lambda(\eta))\Gamma_h(r)/2)}{(\Lambda(\xi)+\Lambda(\eta))\Gamma_h(r)/2}\left(\tfrac{1}{\Lambda(\xi)(\Gamma_h(r)-\tau_h)} + \tfrac{1}{\Lambda(\eta)(\Gamma_h(r)-\tau_h)}\right),\\
&= \tfrac{\Gamma_h(r)(2-\exp(-\Lambda(\xi)\tau_h)-\exp(-\Lambda(\eta)\tau_h))-2\tau_h(1-\exp(-(\Lambda(\xi)+\Lambda(\eta))\Gamma_h(r)/2))}{\tau_h\Gamma_h(r)(\Gamma_h(r)-\tau_h)\Lambda(\xi)\Lambda(\eta)},
\end{aligned}$$

and therefore, using the definitions (5.1) and (5.2), we obtain the results in (5.6) and (5.7). □

Proof of Corollary 6. We find

$$\mathbb{E}[\exp(-\Lambda(\xi)\tau_h)] = \mathbb{E}\Big[\prod_{(c,\gamma)\in\Phi} \exp(-\gamma k(c,\xi)\tau_h)\Big] = \exp(-a(\xi)),$$

where we at the last equality sign have used the form of the generating functional for the Poisson process Φ, see Møller and Waagepetersen (2004, Proposition 3.3). The formula (5.9) is proved in a similar fashion. The result for NSPs is obtained by noting that a NSP is a special case of a SNCP with $k(c,\xi) = k(\xi - c)$ and intensity measure of cluster centres and cluster intensities $\mathrm{d}\zeta(c,\gamma) = \mathrm{d}c\,\mathrm{d}\delta_\mu(\gamma)$, where δ_μ is a measure concentrated in the point μ with $\delta_\mu(\{\mu\}) = \kappa$. □

References

Baddeley, A. and R. Turner (2005, 1). Spatstat: An R package for analyzing spatial point patterns. *Journal of Statistical Software 12*(6), 1–42.

Cox, D. R. (1955). Some statistical methods connected with series of events. *Journal of the Royal Statistical Society. B*(17), 129–164.

Diggle, P. J. (1983). *Statistical Analysis of Spatial Point Patterns*. Academic Press, London.

Fiksel, T. (1988). Edge-corrected density estimators for point processes. *Statistics 19*(1), 67–75.

Hanisch, K.-H. (1982). On inversion formulae for n-fold Palm distributions of point processes in LCS-spaces. *Mathematische Nachrichten 106*(1), 171–179.

Illian, J., A. Penttinen, H. Stoyan, and D. Stoyan (2008). *Statistical Analysis and Modelling of Spatial Point Patterns*, Volume 70. Wiley, Chichester.

Kiderlen, M. and M. Hörig (2013). MatérnŠs hard core models of types I and II with arbitrary compact grains. *CSGB Research Report 05*. Submitted for journal publication.

Lavancier, F. and J. Møller (2015). Modelling aggregation on the large scale and regularity on the small scale in spatial point pattern datasets. *Available at arXiv:1505.07215*. Submitted for journal publication.

Madelung, A. B., H. Bondo, I. Stamp, P. Loevgreen, S. L. Nielsen, A. Falensteen, H. Knudsen, M. Ehinger, R. Dahl-Sørensen, N. B. Mortensen, et al. (2013). World Health Organization-defined classification of myeloproliferative neoplasms: Morphological reproducibility and clinical correlations — the Danish experience. *American Journal of Hematology 88*(12), 1012–1016.

Månsson, M. and M. Rudemo (2002). Random patterns of nonoverlapping convex grains. *Advances in Applied Probability 34*(4), 718–738.

Matérn, B. (1960). Spatial variation. Stochastic models and their application to some problems in forest surveys and other sampling investigations. *Medd. Statens Skogsforskningsinstitut 49*(5), 1–144.

Matérn, B. (1986). *Spatial Variation*. Lecture Notes in Statistics 36, Springer-Verlag, Berlin.

Mattfeldt, T., S. Eckel, F. Fleischer, and V. Schmidt (2006). Statistical analysis of reduced pair correlation functions of capillaries in the prostate gland. *Journal of Microscopy 223*(2), 107–119.

Mattfeldt, T., S. Eckel, F. Fleischer, and V. Schmidt (2007). Statistical modelling of the geometry of planar sections of prostatic capillaries on the basis of stationary Strauss hard-core processes. *Journal of Microscopy 228*(3), 272–281.

Møller, J. (2003). Shot noise Cox processes. *Advances in Applied Probability 35*, 614–640.

Møller, J. and R. P. Waagepetersen (2004). *Statistical Inference and Simulation for Spatial Point Processes*. Chapman and Hall/CRC, Boca Raton, FL.

Neyman, J. and E. L. Scott (1958). Statistical approach to problems of cosmology. *Journal of the Royal Statistical Society. Series B 20*, 1–43.

Stoyan, D. (1979). Interrupted point processes. *Biometrical Journal 21*(7), 607–610.

Stoyan, D., W. S. Kendall, and J. Mecke (1995). *Stochastic Geometry and Its Applications*. Wiley, Chichester, 2nd edition.

Stoyan, D. and H. Stoyan (1985). On one of Matérn's hard-core point process models. *Mathematische Nachrichten 122*(1), 205–214.

Teichmann, J., F. Ballani, and K. G. van den Boogaart (2013). Generalizations of MatérnŠs hard-core point processes. *Spatial Statistics 3*, 33–53.

Thomas, M. (1949). A generalization of Poisson's binomial limit for use in ecology. *Biometrika 36*, 18–25.

Vytrva, N., E. Stacher, P. Regitnig, W. Zinke-Cerwenka, S. Hojas, E. Hubmann, A. Porwit, M. Bjorkholm, G. Hoefler, and C. Beham-Schmid (2014). Megakaryocytic morphology and clinical parameters in essential thrombocythemia, polycythemia vera, and primary myelofibrosis with and without jak2 v617f. *Archives of Pathology & Laboratory Medicine 138*(9), 1203–1209.